Statistical Analysis for Wavelength-Resolution SAR Image Stacks: New Case Studies

Dimas I. Alves, Crístian Müller, Bruna G. Palm Viet T. Vu, Mats I. Pettersson, Renato Machado, and Bartolomeu F. Uchôa-Filho,

***Abstract*— This paper presents new case studies for the statistical analysis for wavelength resolution SAR image stacks. The statistical analysis considers the Anderson-Darling goodness-of-fit test in a set of pixel samples from the same position obtained from a SAR image stack. The test is applied in wavelength-resolution SAR image stacks. The present work consists of two case studies based on the use of multiple-pass stacks and Type I error using the False Discovery Rate controlling procedures. In addition, an application scenario is presented for the studied scenarios.**

***Keywords*— Synthetic Aperture Radar (SAR), wavelength-resolution, image stacks, false discovery rate, FOPEN.**

I. Introduction

Historically, Foliage-Penetrating (FOPEN) applications using Synthetic Aperture Radars (SAR) images, e.g., retrieval of steam volume [2]–[4] and detection of concealed targets [5]–[7], have been of great interest, especially for military and surveillance purposes [8]. In FOPEN applications, when conventional microwave frequency SAR systems are employed, a large number of false alarms are observed caused by the abundance of small scatterers associated with the forest canopy. Ultra High Frequency (UHF) and Very High Frequency (VHF) SAR systems are employed in FOPEN applications to overcome this problem [8]. Both UHF and VHF FOPEN SAR systems are characterized by their large fractional bandwidth and a wide antenna bandwidth. These characteristics result in systems resolutions in the order of the radar signal wavelengths [9]. Hence, the images generated by this kind of system are frequently called wavelength-resolution images.

The backscattering phenomenology for wavelength-resolution SAR systems is different from traditional microwave SAR. For wavelength-resolution systems, target-size elements have the characteristic of a resonance scattering regime, whereas small objects present the characteristic of a Rayleigh scattering regime [10]. Thus, the contribution of small scatterers present in the ground area of interest is very limited for wavelength-resolution SAR systems. The scattering process is mainly related to scatterers with dimensions in the order of the signal wavelengths. For instance, in a forestry area scenario with a VHF SAR system, the foliage backscatter is dominated by the direct and ground-reflected backscattering from tree stems [11]. Therefore, there might be only a single scatter in the resolution cell. As a consequence, the image will not suffer from speckle noise. The large scatterers in a ground area of interest tend to be static objects, which are frequently less sensitive to weather conditions than small scatterers. Large scatterers tend to be stable in time. Therefore, it is possible to obtain highly similar images of a determined area by measuring with multi-passes [12].

Based on these observations, wavelength-resolution systems are an adequate selection for FOPEN applications, and several studies using data from those systems have been carried out in the last decades [13]–[17]. Several recent publications [18]–[20] shows that the performance gain in terms of false alarm occurrence in change detection methods for wavelength-resolution SAR images can be achieved by considering the use of small image stacks. Although, the use of image stacks in high-resolution SAR images is a well-studied topic [21], [22], their use in change detection applications using wavelength-resolution SAR images has not yet been well explored.

Recently, an initial study related to the background statistics in wavelength-resolution SAR image stacks has been implemented, which provided some insights that can be useful for change detection methods [1]. Motivated by the results presented in [1], this paper presents two case studies for the statistical test analysis presented in [1]. The case studies consist of the use of multiple passes stacks and Type I error using False Discovery Rate (FDR) controlling procedures. The discussions related to the background statistics and changes behavior in wavelength-resolution SAR image stacks and simple change detection scenario are presented for both case studies.

The remainder of this paper is organized as follows. The information related to the CARABAS II data set, used throughout this paper, is provided in Section II. A brief discussion of the statistical test analysis, presented in [1], for wavelength-resolution SAR image stacks, is presented in Section III. Section IV presents the extension of the statistical test analysis, which consists of two study case evaluations. Moreover, one application scenario for the case studies is presented. Finally, Section V presents some concluding remarks.

Dimas Irion Alves and Crístian Müller¸ Federal University of Pampa (UNIPAMPA), Alegrete - RS, Brazil. Email: (dimasalves, cristianmuller)@unipampa.edu.br.; Viet T. Vu, Mats I. Pettersson, Blekinge Institute of Technology (BTH), Karlskrona, Sweden. Email: (viet.thuy.vu, mats.pettersson)@bth.se; Bruna G. Palm and Renato Machado, Aeronautics Institute of Technology (ITA), São José dos Campos, Brazil. Email: brnagpalm@gmail.com and rmachado@ita.br; Bartolomeu F. Uchôa-Filho¸ Universidade Federal de Santa Catarina, Florianópolis, Brasil, E-mail: uchoa@eel.ufsc.br.

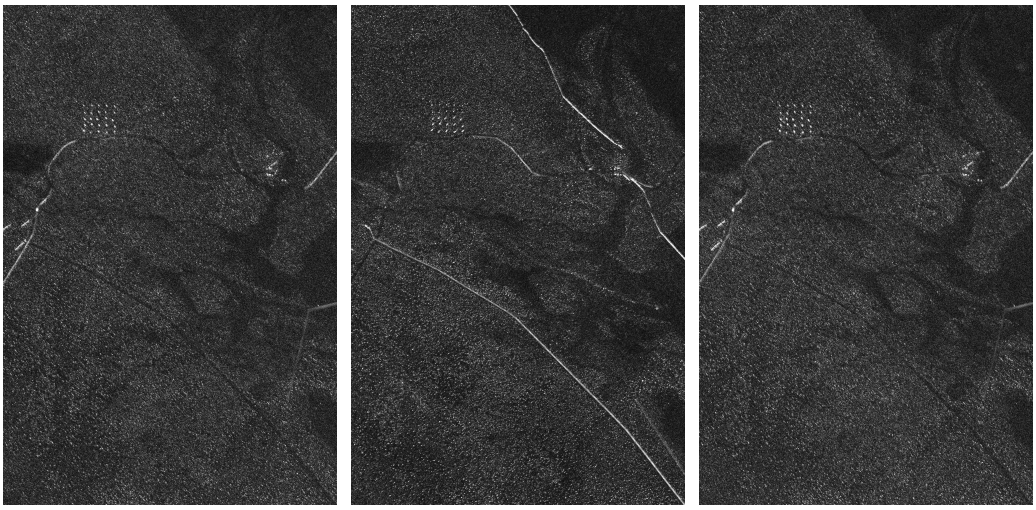

(a) (b) (c)

Fig. 1. CARABAS II images obtained for (a) Stack 1, (b) Stack 2, and (c) Stack 3.

II. Data Description

The data set considered in this study is composed of 24 incoherent SAR images from a set of 150 SAR images obtained during a flight campaign in the Missile Test Range North (RFN), in Vidsel, in northern Sweden [23]. The selected test sites are regions dominated by small/medium-sized trees, in which the dominant species is the Scots pine. However, there is also the presence of lakes, fields, and other structures, such as roads, fences, and power lines. Each image covers the same ground area of 6 km^2 (2 km $\times$ 3 km) and is given in the form of a 3000 $\times$ 2000 matrix, where the pixel size is 1 m $\times$ 1 m and the images are already calibrated, pre-processed, and geocoded.

The 24 images are divided into four target deployments (Missions), which are measured using different flight geometries (Passes). Also, the images can be equally divided into three stacks according to their flight geometry. The images obtained with Passes 1 and 3 form Stack 1, while Stack 2 is formed by images obtained with Passes 2 and 4; the rest builds Stack 3. The image samples of each stack are presented in Figure 1.

III. Statistical Test Analysis

The statistical test analysis presented in [1] is briefly described in this section and will be used as a reference for the case studies considered in this paper. Given the scattering and statistical properties of wavelength-resolution images, the statistical test analysis is made between pixels from different measurements of the same stack.

As previously mentioned, each stack contains eight images with six million pixels per image. Thus, the available information for the statistical test in the evaluated position is related to eight amplitude values. However, performing the statistical analysis with only eight samples is inappropriate. Thus, eight additional surrounding pixels (around the tested pixel) are also considered in the statistical analysis. This selection is based on the CARABAS II system spatial resolution, which is about 3 m $\times$ 3 m. Hence, the statistical test analysis is performed in each one of the 6 million positions using 8 $\times$ 9 pixels samples for each evaluation.

The statistical test analysis consists of applying the widely used statistical nonparametric Anderson Darling (AD) Goodness-of-Fit (GoF) test in all pixel positions considering the previously mentioned data samples. The AD test aims to determine if a given null hypothesis (H_0) would be rejected [24]. Hence, the AD test can be used to investigate if a given probability distribution null hypothesis should be rejected for a given sample data. For the sake of simplicity and better use of computational resources, the AD test implementation and approximations presented in [25] are considered throughout this paper.

A. Previous Results

According to the discussion provided in [1], regarding the statistical test analysis, a relation between the presence of changes in the image(s) of a stack and the rejection of the Rician distribution null hypothesis in the AD GoF test can be established. Furthermore, the Rician distribution yielded the best fit for the test data set among the evaluate candidate distributions in [1]. The statistical test failed to reject the Rician distribution for approximately 98% in all the evaluated stacks. Due to it, throughout this paper, only the Rician distribution null hypothesis is considered. One example of the statistical test output is presented as a binary image in Figure 2, where the target deployments areas and the back-lobe structures are highlighted in red and blue, respectively.

As can be observed in Figure 2, all targets are visible inside the red areas. Additionally, back-lobe structures are visible inside the blue area; these structures are related to systems or image formation issues and have similar behavior as regular changes. Usually, different processing techniques are required to remove this type of structure responses; however, it is a

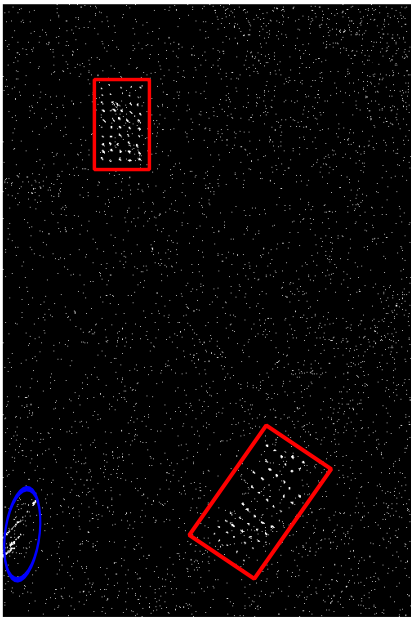

Fig. 2. The AD GoF test results for one image stack, where the target deployment areas, and the back-lobe structures are highlighted inside the red and blue marks, respectively. Passes 1 and 3 were considered for this evaluation.

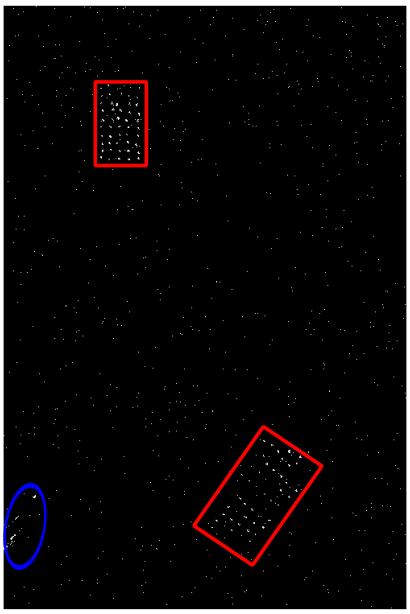

Fig. 3. The AD GoF test results for the concatenated image stack, where the target deployment areas, and the back-lobe structures are highlighted inside the red and blue marks, respectively. Passes 1, 3, 5, and 6 were considered for this evaluation.

topic outside of this paper scope. We can also observe the isolated false discoveries in several image regions.

It is important to emphasize that, the discussions related to the correlation among the tested pixels and their neighbors, and the use of Type I error control techniques are just marginal in [1]. Thus, to provide a more in-depth evaluation of the statistical test, further discussions will be given in Section IV-A and IV-B.

IV. Case Studies

A. Multiple-Passes Stacks

The tested scenario presented in [1] is not ideal, given the necessity of the use of the pixel neighbors. These pixel samples tend to have some degree of correlation with the pixel under evaluation. A higher number of images with the same flight geometries would be required to avoid the use of the pixel neighbors, resulting in a more accurate scenario for the statistical test analysis.

Under the limitations of the CARABAS II data set, it is not possible to obtain more than eight images with the same flight geometries. However, one can consider that wavelength-resolution images obtained with slightly different flight geometries tend to have similar statistics, due to their scattering properties. Since Stacks 1 and 3 share similar flight geometries, it is possible to merge them into a larger stack, resulting in a total of 16 available images. Hence, the statistical test described in Section III is applied to the merged stack without considering the use of pixel neighbors. The results of the test are presented in the form of a binary image in Figure 3, where the target deployments areas and the back-lobe structures are highlighted in red and blue, respectively.

The experimental results show that the AD GoF test fails to reject the null hypotheses of the Rician distribution in 99.67% of the tested samples. This result is similar to the ones observed in [1] and Section III, from which it is possible to state that the Rician distribution yields a good fit for clutter statistics in wavelength-resolution SAR image stacks, even considering slightly different flight geometries. The relation between the presence of changes in the image(s) of a stack and groups of null hypotheses rejections remains. It is possible to state that if stacks with clearly different flight geometries are combined, e.g., Stacks 1 and 2, or 2 and 3, the different clutter structures observable in Figure 1 would be treated as changes. Thus, the use of image stacks with images from different passes may result in totally unexpected observations, especially with the increase of flight geometries discrepancies.

B. Type I Error Control Technique - False Discovery Rate

The presented statistical analysis in [1] is related to a multi-comparison scenario. Thus, an increase in the occurrence of isolated false positives (Type I errors) is expected [26]. In the majority of the cases, this is not a problem in wavelength-resolution applications, given that, due to scattering properties of the images, isolated detections are frequently removed in the application processing chain [23], [27]. However, this scenario may be considered in applications where no removal of isolated objects is applied.

In those situations, Type I error control techniques may be applied, such as Bonferroni correction, Family-wise error rate control, and false discovery rate control [26], [28]. However, it is not possible to control Type I errors and false-negative occurrences (Type II errors), simultaneously [29]. Additionally, most Type I error control techniques could

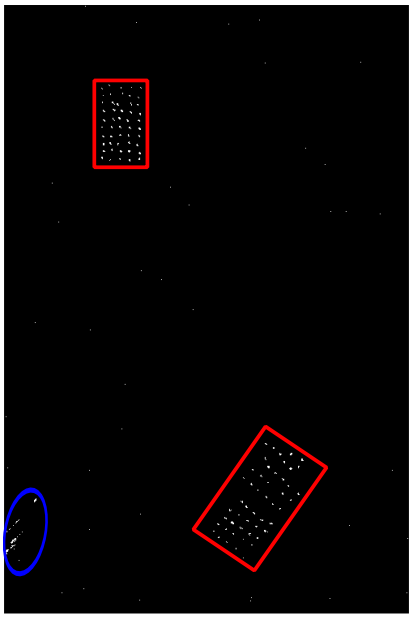

Fig. 4. The AD GoF test results for one image stack using the FDR control technique, where the target deployment areas, and the back-lobe structures are highlighted inside the red and blue marks, respectively. Passes 1 and 3 were considered for this evaluation.

be statistically too conservative, considering the number of multiple tests performed. Based on the characteristics of the error control techniques, the FDR technique proposed in [26] is considered for this study case.

The FDR technique proposed in [26], controls the FDR at a level q and consists of rejecting the null hypothesis for all $H_{(i)}$ where $i = 1 \dots k$. The largest value k can be retrieved from the following condition

$$P_{(k)} \leq \frac{k}{m} q, \tag{1}$$

where $P_{(1)} \dots P_{(m)}$ are the corresponding p-values sorted in an ascending order, m is the total number of tests, and $q = 0.05$. The results of the test for one stack is presented in the form of a binary image in Figure 4, where the target deployments areas and the back-lobe structures are highlighted in red and blue, respectively.

The experimental results show that the AD GoF test using the FDR control technique fails to reject the null hypothesis on the Rician distribution in 99.86% of the tested samples. As can be observed, similar observations as made in Section IV and [1] can be drawn. Additionally, a smaller number of discoveries were observed, which tend to reduce the false alarm occurrence when applied into change detection applications. However, it may jeopardize the detection probability in these applications. These aspects are further discussed in the following section.

C. Application Scenario

To exemplify possible scenarios where the proposed methodology using wavelength-resolution SAR images can be applied, a simple change detection algorithm is presented. The change detection procedure consists of applying one morphological operation of erosion and dilatation in the desired output binary image of the GoF test to remove isolated detections. The operations consider the use of one structuring element size equals to the system resolution cell [23], [27]. It is important to emphasize that, due to the scattering process of wavelength-resolution images, it is not expected to erase any target in this process. After that, a multiplication process is performed where the surveillance image pixels are multiplied with the output binary image in the same position. Then, thresholding is performed.

For the sake of simplicity, a threshold (τ) was selected considering $P(z_s < \tau) = 99\%$, where z_s represents the amplitude of the surveillance image. The thresholding process assigns 1 to the pixels with amplitudes above the fixed threshold, whereas the other pixels are assigned 0. Finally, to avoid the appearance of fragmented objects, a final dilatation is performed in the output image merging the adjacent detected pixels, within a distance lower than 10 m. A performance comparison, considering the previously evaluated stacks and case studies, is performed, and the results are presented in Figure 5.

As can be observed in Figure 5, even with a very simple processing chain, the change detection method considering both case studies was able to detect 24 out of 25 targets without any false alarm. However, there are targets that have been erased, as can be seen in sub-figures a) and b), resulting in the inability of detecting them, independently of the used surveillance image. Moreover, the simple processing scheme was unable to deal with the back-lobe structures that, when present in the surveillance image, are detected as targets.

Based on the results, some remarks can be drawn. Firstly, the use of image stacks in wavelength-resolution change detection methods present a proper functioning and deserve further studies. The use of Type I error control techniques showed the capability to remove some of the isolated detections, which tends to reduce the occurrence of false alarms. However, its use may prevents detecting some targets.

V. Concluding Remarks

This paper presented two study case scenarios for the previously published statistical test analysis considering wavelength-resolution SAR image stacks. The results presented in this paper corroborate with the affirmation that the Rician distribution yields a good fit for the background statistics in wavelength-resolution SAR image stacks. Also, a relation between changes in image stacks and the rejection of the Rician distribution null hypothesis in the AD GoF test was observed. Additionally, a simple change detection processing chain was presented. Based on the results obtained, the use of image stacks worked properly and granted suitable performance.

Acknowledgment

This work was partially supported by the Brazilian National Council for Scientific and Technological Development (CNPq), Coordination for the Improvement of Higher Education Personnel (CAPES), by the Swedish-Brazilian Research and Innovation Centre (CISB) and by Saab AB.

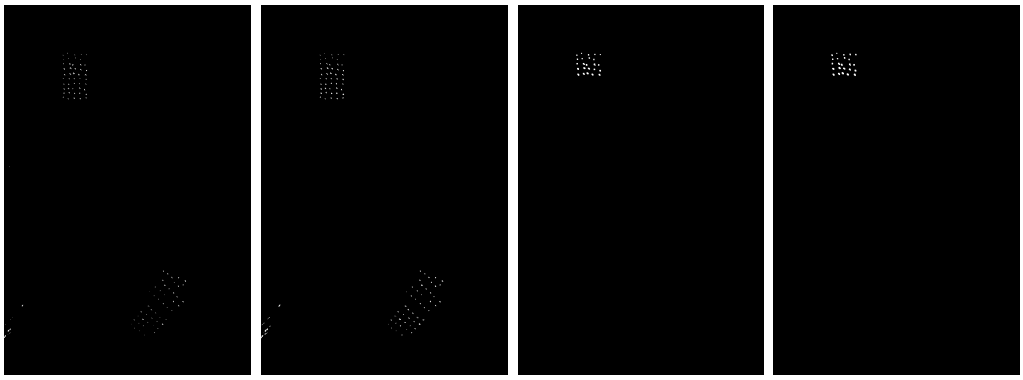

Fig. 5. Output binary images after the morphological operations a) using the concatenated stack; b) using the FDR technique, and change detection scenario: c) using the concatenated stack; d) using the FDR technique. The same passes were considered for each scenario.

REFERENCES

[1] D. I. Alves, B. G. Palm, M. I. Pettersson, V. T. Vu, R. Machado, B. F. Uchôa-Filho, P. Dammert, and H. Hellsten, "A statistical analysis for wavelength-resolution SAR image stacks," *IEEE Geoscience and Remote Sensing Letters*, vol. 17, no. 2, pp. 227–231, Feb. 2020.

[2] H. Israelsson, L. M. H. Ulander, J. L. H. Askne, J. E. S. Fransson, P.-O. Frolind, A. Gustavsson, and H. Hellsten, "Retrieval of forest stem volume using vhf SAR," *IEEE Transactions on Geoscience and Remote Sensing*, vol. 35, no. 1, pp. 36–40, Jan. 1997.

[3] P. Melon, J. M. Martinez, T. L. Toan, L. M. H. Ulander, and A. Beaudoin, "On the retrieving of forest stem volume from VHF SAR data: observation and modeling," *IEEE Transactions on Geoscience and Remote Sensing*, vol. 39, no. 11, pp. 2364–2372, Nov. 2001.

[4] K. Folkesson, G. Smith-Jonforsen, and L. M. H. Ulander, "Model-based compensation of topographic effects for improved stem-volume retrieval from CARABAS-II VHF-band SAR images," *IEEE Transactions on Geoscience and Remote Sensing*, vol. 47, no. 4, pp. 1045–1055, Apr. 2009.

[5] L. M. H. Ulander, W. E. Pierson, M. Lundberg, P. Follo, P.-O. Frolind, and A. Gustavsson, "Performance of VHF-band SAR change detection for wide-area surveillance of concealed ground targets," in *SPIE Defense and Security Symposium: Algorithms for Synthetic Aperture Radar Imagery XI*, vol. 5427, 2004.

[6] Z. Wei, G. Jian, and W. Jie, "Change detection of concealed targets using repeat-pass SAR images," in *1st Asian and Pacific Conference on Synthetic Aperture Radar*, Nov. 2007, pp. 275–278.

[7] L. M. H. Ulander, B. Flood, P.-O. Frolind, A. Gustavsson, T. Jonsson, B. Larsson, M. Lundberg, D. Murdin, and G. Stenstrom, "Change detection of vehicle-sized targets in forest concealment using VHF- and UHF-band SAR," *IEEE Aerospace and Electronic Systems Magazine*, vol. 26, no. 7, pp. 30–36, Jul. 2011.

[8] W. L. Melvin and J. A. Scheer, *Principles of Modern Radar: volume III - Radar Applications*, 1st ed. Edison, USA: SciTech Publishing, 2014.

[9] H. Hellsten, L. M. H. Ulande, A. Gustavsson, and B. Larsson, "Development of VHF CARABAS II SAR," in *Radar Sensor Technology*, Apr. 1996, pp. 48–60.

[10] L. M. H. Ulander, "VHF-band SAR for detection of concealed ground targets," in *RTO SCI Symposium on Sensors and Sensor Denial by Camouflage, Concealment and Deception*, 2004, pp. 1–11.

[11] G. Smith and L. M. H. Ulander, "A model relating VHF-band backscatter to stem volume of coniferous boreal forest," *IEEE Transactions on Geoscience and Remote Sensing*, vol. 38, no. 2, pp. 728–740, Mar. 2000.

[12] R. Machado, V. T. Vu, M. I. Pettersson, P. Dammert, and H. Hellsten, "The stability of UWB low-frequency SAR images," *IEEE Geoscience and Remote Sensing Letters*, vol. 13, no. 8, pp. 1114–1118, Aug. 2016.

[13] K. N. L. Priya, R. Nagendran, and A. Sreedevi, "Detection of foliage covered immobile targets based on incoherent change detection and SURE," in *2012 International Conference on Communications, Devices and Intelligent Systems (CODIS)*, Dec. 2012, pp. 389–392.

[15] Y. C. Liu, G. X. Wang, P. Li, and X. P. Yan, "Unsupervised sar change detection based on a new statistical model," in *IET International Radar Conference 2015*, 2015, pp. 1–4.

[14] W. Ye, C. Paulson, D. O. Wu, and J. Li, "A target detection scheme for VHF SAR ground surveillance," in *SPIE Defense and Security Symposium: Algorithms for Synthetic Aperture Radar Imagery XV*, vol. 6970.

[16] M. Liguori, A. Izzo, C. Clemente, C. Galdi, M. D. Bisceglie, and J. Soraghan, "A location scale based CFAR detection framework for FOPEN SAR images," in *2015 Sensor Signal Processing for Defence (SSPD)*, 2015, pp. 1–5.

[17] M. I. Pettersson, V. T. Vu, N. R. Gomes, P. Dammert, and H. Hellsten, "Incoherent detection of man-made objects obscured by foliage in forest area," in *2017 IEEE International Geoscience and Remote Sensing Symposium (IGARSS)*, 2017, pp. 1892–1895.

[18] V. T. Vu, M. I. Pettersson, R. Machado, P. Dammert, and H. Hellsten, "False alarm reduction in wavelength-resolution SAR change detection using adaptive noise canceler," *IEEE Transactions on Geoscience and Remote Sensing*, vol. 55, no. 1, pp. 591–599, Jan. 2017.

[19] V. T. Vu, "Wavelength-resolution SAR incoherent change detection based on image stack," *IEEE Geoscience and Remote Sensing Letters*, vol. 14, no. 7, pp. 1012–1016, Jul. 2017.

[20] B. G. Palm, D. I. Alves, M. I. Pettersson, V. T. Vu, R. Machado, R. J. Cintra, F. M. Bayer, P. Dammert, and H. Hellsten, "Wavelength-resolution SAR ground scene prediction based on image stack," *Sensors*, vol. 20, no. 7, Apr. 2020.

[21] F. Baselice, G. Ferraioli, and V. Pascazio, "Markovian change detection of urban areas using very high resolution complex SAR images," *IEEE Geoscience and Remote Sensing Letters*, vol. 11, no. 5, pp. 995–999, May 2014.

[22] Y. Wang, X. X. Zhu, and R. Bamler, "An efficient tomographic inversion approach for urban mapping using meter resolution SAR image stacks," *IEEE Geoscience and Remote Sensing Letters*, vol. 11, no. 7, pp. 1250–1254, Jul. 2014.

[23] M. Lundberg, L. M. H. Ulander, W. E. Pierson, and A. Gustavsson, "A challenge problem for detection of targets in foliage," in *SPIE Defense and Security Symposium: Algorithms for Synthetic Aperture Radar Imagery XIII*, vol. 6237, May 2006.

[24] T. W. Anderson and D. A. Darling, "Asymptotic theory of certain "goodness of fit" criteria based on stochastic processes," *Annals of Mathematical Statistics*, vol. 23, no. 02, pp. 193–212, Jun. 1952.

[25] G. Marsaglia and J. C. W. Marsaglia, "Evaluating the anderson-darling distribution," *Journal of Statistical Software*, vol. 9, no. 2, pp. 1–5, Feb. 2004.

[26] B. Yoav and H. Yosef, "Controlling the false discovery rate: A practical and powerful approach to multiple testing," *Journal of the Royal Statistical Society. Series B (Methodological)*, vol. 57, no. 1, pp. 289–300, Aug. 1995.

[27] L. M. H. Ulander, M. Lundberg, W. Pierson, and A. Gustavsson, "Change detection for low-frequency SAR ground surveillance," *IEE Proceedings - Radar, Sonar and Navigation*, vol. 152, no. 6, pp. 413–420, Dec. 2005.

[28] V. A. Krylov, G. Moser, S. B. Serpico, and J. Zerubia, "False discovery rate approach to unsupervised image change detection," *IEEE Transactions on Image Processing*, vol. 25, no. 10, pp. 4704–4718, Oct. 2016.

[29] S. M.Kay, *Fundamentals of Statistical Signal Processing. Detection Theory*, 1st ed. New Jersey, USA: Prentice-Hall, 1989.